Building and Environment, Vol. 24, No. 1, pp. 65–72, 1989.
Printed in Great Britain.

0360–1323/89 $3.0(

Numerical Simulations of Pressure Fields Around Buildings

KENNETH HÄGGKVIST*
URBAN SVENSSON*
ROGER TAESLER*

Numerical calculations of the pressure field around a small-scale house have been performed. The calculations are simulations of wind tunnel experiments, and the flow conditions in the wind tunnel were reproduced as accurately as possible. The results indicate that, for engineering purposes, the numerical model does give relevant information about the flow and pressure fields around buildings with rather complicated geometry. An analysis of the results further indicates that the calculations can be improved in a fairly straightforward fashion with refined boundary conditions.

1. INTRODUCTION

COMMON PROCEDURES to obtain a realistic description of the flow and pressure field around 3-D obstacles, such as different kinds of buildings, are to undertake full scale measurements and experiments, i.e. wind tunnel studies. Full scale, or field measurements, suffer from a lack of generality and are expensive. Wind tunnel studies are carried out under controlled experimental conditions and results of a certain generality are therefore possible to obtain. Wind tunnel experiments are, however, rather time consuming and relatively expensive.

Modern computational fluid dynamics models in combination with powerful computers offer an additional, or in some cases, an alternative way to study building related flow problems. These are not trivial, as realistic simulations of the flow field around a building accentuate the need for a good description of the turbulent processes in front, above and behind a 3-D building. An advanced modelling of the turbulent processes is therefore necessary in the numerical models which are going to be used.

A brief survey of the literature confirms that the numerical modelling approach will provide an alternative to field or laboratory measurements in the near future. Hanson *et al.* [1] investigated two different methods, a random vortex method and a control volume method, in a 2-D analysis of the flow over a building. Later, Summers *et al.* [2], extended their control volume method to three dimensions and compared the predictions with laboratory measurements. The agreement was generally good but the shape of the wake region was poorly predicted. This may be due to the representation of turbulence in the model [2]. A constant eddy viscosity was used, which is probably inadequate in the wake region. Paterson and Apelt [3] used the k–ε model together with the Reynolds equation and the continuity equation in their 3-D model. The k–ε model is known, see Rodi [4], to give an eddy viscosity field which is adequate for engineering purposes. Paterson and Apelt also concluded that good agreement with full scale and wind tunnel measurements was obtained generally.

In this paper numerical simulations concerning the pressure distribution on a small house are presented and discussed. The calculations have been done with the general equation solver PHOENICS (Spalding [5]), using the standard k–ε turbulence model. The calculations are simulations of wind tunnel experiments performed at SIB, the Swedish Institute of Building Research, and presented by Wirén [6].

2. THE NUMERICAL EXPERIMENTS

2.1. *General*

In the numerical experiments the different properties of the wind tunnel studies were reproduced as accurately as possible. The geometric measurements of the building were the same as in the wind tunnel experiments. The initial conditions were not critical for the problem, since steady state problems were studied. The boundary conditions that were applied in the numerical calculations were vertical profiles of the horizontal velocity, the turbulent kinetic energy and its dissipation rate. The profiles were obtained in the wind tunnel measuring section, without any disturbing house(s) placed in the air flow. No attempt to model the different mechanical turbulence generating arrangements in the wind tunnel was made.

In Figs 1a and b the houses studied are shown, namely a single house and a house surrounded by a number of identical houses in a symmetrical pattern. For each case two wind directions were investigated, namely wind against the long side of the house and against the gable wall, as indicated in Fig. 1.

2.2. *Geometrical representation of the house*

In Fig. 2 the numerical representation of the house is shown. The roof of the house was modelled in a stepwise fashion. The symmetrical properties of the house configurations showed in Fig. 1, have been used as far as

*The Swedish Meteorological and Hydrological Institute (SMHI), Norrköping, Sweden.

BAE 24/1-E

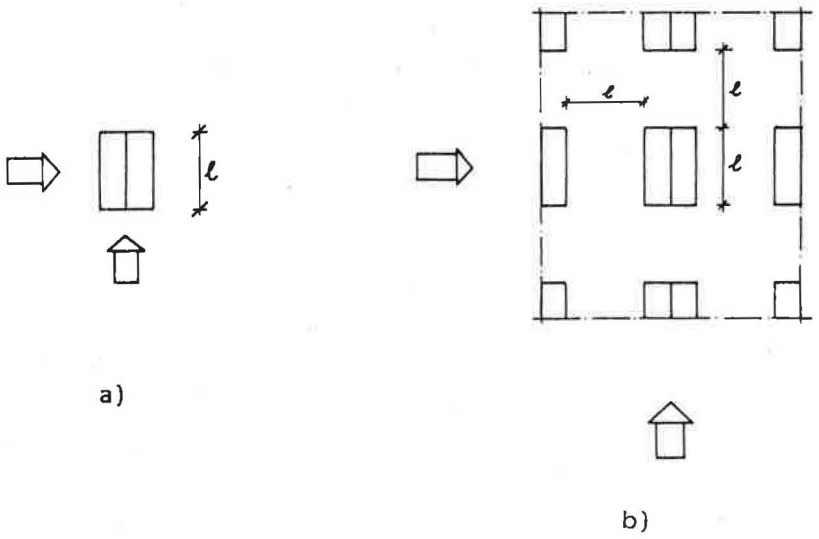

Fig. 1. The house configurations investigated: (a) a single house; (b) a house surrounded by identical houses.

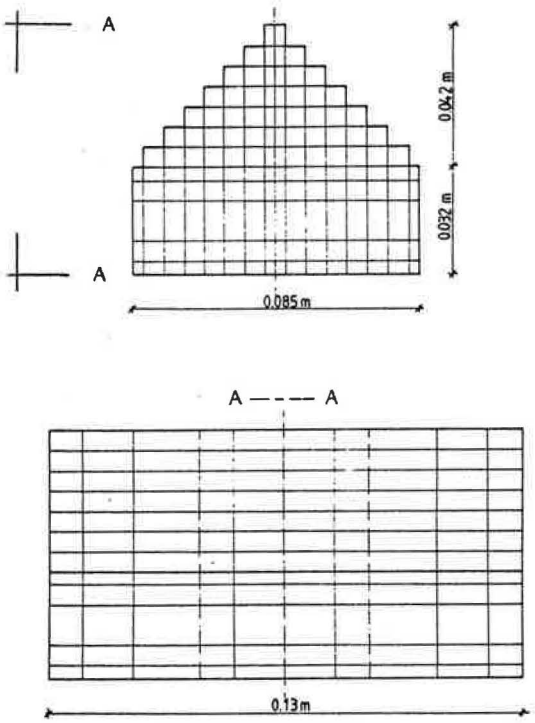

Fig. 2. The numerical representation of the house.

possible. For the single house the calculation domain was about 14 house heights (h) high, the distance from the domain inlet (vertical) boundary to the house was about $5h$ and the downstream distance to the domain outlet boundary was about $12h$. These figures were based partly on literature data concerning numerical and experimental 2-D tests, and partly on data from a few test runs within this work. In Fig. 3 the single house with its calculation domain is shown. In this case it was important to make the domain large enough to avoid interaction between the recirculation zones and the boundaries. In the case of a group of symmetrically located houses, the lateral boundaries were fixed by the distance between the houses, i.e. the interaction between the recirculation zones and the boundaries were essential parts of the problem. The top of the calculation domain was in this case situated at the same distance above the "floor" as for the single house, that is about $14h$, as shown in Fig. 4.

2.3. *Differential equations and their solution*

The equations governing the flow around buildings are based on the principles of conservation of mass, momentum and energy. For an incompressible flow we may derive the Navier–Stokes equation and the continuity equation from these principles. For a steady-state problem we may further define an average and a fluctuating velocity component at each point and coordinate direction, the so called Reynolds decomposition. If this decomposition is introduced into the equations and the equations are then time-averaged, the following mean flow equations result:

Momentum:

$$U_j \frac{\partial U_i}{\partial x_j} = -\frac{1}{\rho}\frac{\partial p}{\partial x_i} + \frac{\partial}{\partial x_j}\left(\nu \frac{\partial U_i}{\partial x_j} - \overline{u_i u_j}\right), \quad i = 1,2,3 \qquad (1)$$

Continuity:

$$\frac{\partial U_j}{\partial x_j} = 0, \qquad (2)$$

where U_i is the mean velocity, p pressure, ν kinematic laminar viscosity, ρ density, x_i coordinate direction and $\overline{u_i u_j}$, the Reynolds stress tensor.

A turbulence model is required for the Reynolds stress tensor. The first step is to introduce the eddy viscosity by the following relation (the Boussinesq eddy viscosity concept):

$$-\overline{u_i u_j} = \nu_T \left(\frac{\partial U_i}{\partial x_j} + \frac{\partial U_j}{\partial x_i}\right) - \frac{2}{3} k \delta_{ij}, \qquad (3)$$

where ν_T is the kinematic eddy-viscosity, k the turbulent kinetic energy ($= 1/2(\overline{u_1^2} + \overline{u_2^2} + \overline{u_3^2})$ and δ_{ij} the Kronecher delta, Equation (3) can be regarded as a definition of the

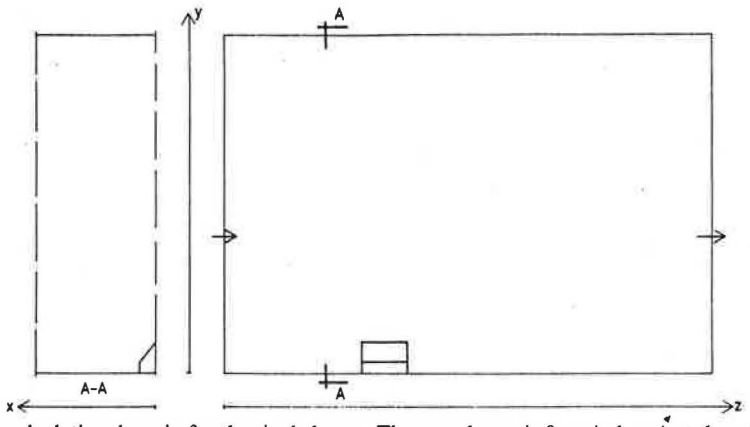

Fig. 3. The calculation domain for the single house. The case shown is for wind against the gable wall.

eddy viscosity and the problem is now to find a model for ν_T. The k–ε model, which is to be used in this investigation, makes use of the Prandtl–Kolmogorov relation in order to express ν_T in terms of k and ε, where ε is the dissipation rate of k. This relation reads:

$$\nu_T = c_\mu \frac{k^2}{\varepsilon}, \tag{4}$$

where c_μ is an empirical coefficient. In order to close the system of equations, k and ε need to be determined. Exact equations for these variables can be derived from the basic conservation principles. These equations are then modelled, through a combination of dimensional analysis, experimental data and physical insight, with the following result:

k-equation:

$$U_j \frac{\partial k}{\partial x_j} = \frac{\partial}{\partial x_j}\left(\frac{\nu_T}{\sigma_k}\frac{\partial k}{\partial x_j}\right) + P - \varepsilon, \tag{5}$$

ε-equation:

$$U_j \frac{\partial \varepsilon}{\partial x_j} = \frac{\partial}{\partial x_j}\left(\frac{\nu_T}{\sigma_\varepsilon}\frac{\partial \varepsilon}{\partial x_j}\right) + C_{1\varepsilon}\frac{\varepsilon}{k}P - C_{2\varepsilon}\frac{\varepsilon^2}{k}, \tag{6}$$

$$P = \nu_T\left(\frac{\partial U_i}{\partial x_j} + \frac{\partial U_j}{\partial x_i}\right)\frac{\partial U_i}{\partial x_j}, \tag{7}$$

where P is the production of k, σ_k and σ_ε Prandtl/Schmidt numbers and $C_{1\varepsilon}$ and $C_{2\varepsilon}$ are empirical coefficients. A detailed account of the k–ε model can be found in Rodi [4].

Equations (1–7) were solved using the general equation solver PHOENICS [5]. PHOENICS is based on a control volume technique and solves the equations in a fully implicit manner.

2.4. *Initial and boundary conditions*

For the case of the single house, the initial conditions were of secondary interest, as the problem was a steady-state one. The boundary conditions were quite straightforward, at the "floor" the law of the wall was applied and at the outlet boundary zero pressure prevailed. The inlet boundary conditions concerning horizontal velocity, the turbulent kinetic energy, k, and its dissipation rate, ε, were specified via vertical profiles close to the measured profiles. In Fig. 5 the profiles for the horizontal velocity and the turbulence intensity are shown. The inlet profiles of k and ε were calculated as

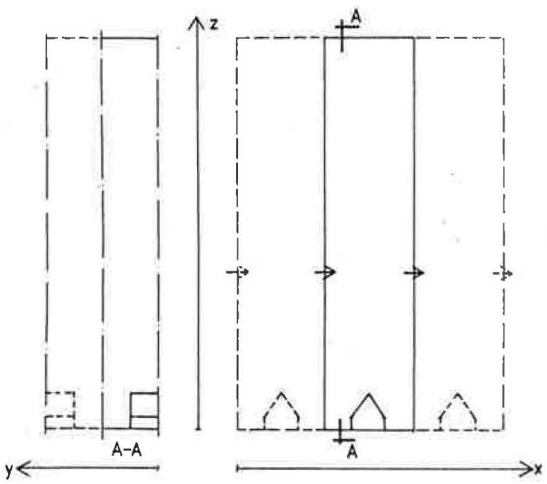

Fig. 4. The calculation domain for the house in a group of identical houses. The case shown is for wind against the longside wall.

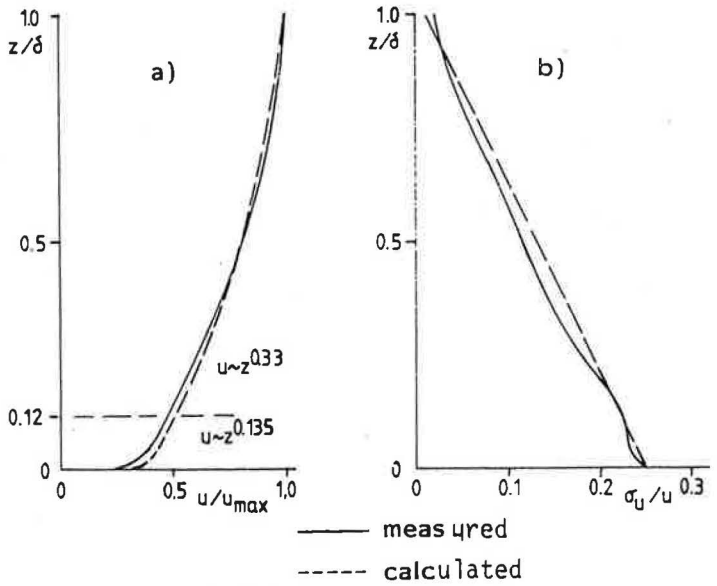

Fig. 5. Vertical profiles of horizontal velocity and horizontal turbulence intensity. The wind tunnel measurements are taken from [6].

follows. The turbulence intensity, according to Fig. 5b, can be approximated by:

$$\sigma_u/\bar{u}(z) = 0.247 - 0.235z/\delta, \tag{8}$$

where z = vertical distance from the "floor" and δ = height of the wind tunnel boundary layer; k is given by the expression:

$$k = \tfrac{1}{2}(\overline{u'^2} + \overline{v'^2} + \overline{w'^2}), \tag{9}$$

and:

$$\overline{u'^2} = \sigma_u^2\,;\ \overline{v'^2} = \sigma_v^2\,;\ \overline{w'^2} = \sigma_w^2.$$

If the turbulence is not isotropic, as is probably the case in boundary layers, Zeman and Tennekes [7] have shown that:

$$\overline{u'^2} \simeq 1.08k. \tag{10}$$

This gives the expression for the turbulent kinetic energy, which has been used as the inlet boundary condition:

$$k(z) = \frac{\sigma_u^2}{1.08} = ((0.247 - 0.235z/\delta)\bar{u}(z))^2/1.08. \tag{11}$$

The dissipation rate of the turbulent kinetic energy, ε, can be written:

$$\varepsilon = c_D k^{3/2}/L \tag{12}$$

where c_D is the dissipation coefficient and L is a length scale. Transforming L to a relevant boundary layer mixing length scale [4] gives:

$$\varepsilon(z) = 0.41k(z)^{3/2}/z, \tag{13}$$

where $k(z)$ is given by Equation (11). The conditions at the "floor" for the different variables were given by the wall laws [4].

Concerning the house situated in a group of identical houses, the initial fields for the horizontal velocity, k and ε were those given by Fig. 5a and Equations (11) and (13). The inlet boundary conditions for a certain iteration (sweep) were in this case generated by the outlet conditions in the foregoing iteration. The PHOENICS code has an option for cyclic boundary conditions, which was used to generate this effect. At the top of the flow domain the horizontal velocity, k and ε were set to constant values, given by Fig. 5a and Equations (11) and (13). This manner used to prescribe the top boundary conditions is somewhat questionable but is not believed to influence the region of interest. At the lateral boundaries, parallel to the main flow, the conditions were of the symmetry type and the wall condition was applied at the "floor".

3. RESULTS

3.1. *General*

The results from the numerical calculations are presented in three ways. Firstly, the pressure distribution on the different house areas, long side, gable and roof, are presented as pressure coefficient isoplots. Second, the wind tunnel results were presented as pressure coefficient distributions at one horizontal level and vertical section on the house. From the numerical calculations corresponding pressure values have been drawn in order to make a direct comparison with the wind tunnel pressure distribution possible. The third presentation is the average pressure for each wall of the house, numerically calculated versus measured.

The pressure values used in the presentations are not the absolute ones, as dimensionless pressure coefficients are usually used in these studies. In this work the pressure coefficient is defined as:

$$c_p = ((p(x,y,z) - p_{ref})/(0.5\rho u_{ref}^2), \tag{14}$$

where $p(x,y,z)$ = actual pressure at a gridpoint; p_{ref} = a reference pressure, here the pressure at the wind tunnel roof level above the house; ρ = density of air; u_{ref} = reference velocity, here the horizontal velocity at house roof top level, according to the profile in Fig. 5a. The coefficient definition (Equation (14)), agrees with the pressure coefficient used in the wind tunnel experiments.

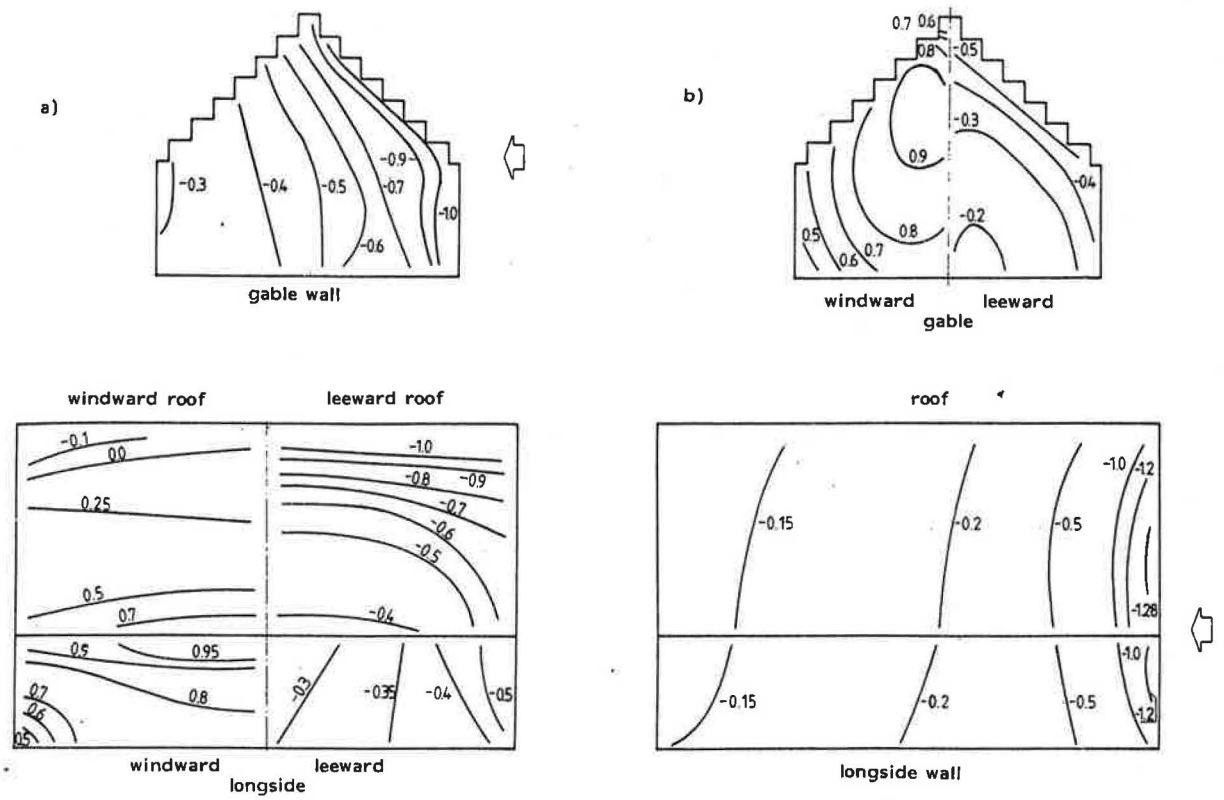

Fig. 6. Predicted distribution of the pressure coefficient (c_p), on the surface of a single house. Wind direction: (a) towards the longside wall; (b) towards the gable wall.

The calculated and measured pressures are thus comparable.

3.2. *The single house*

In Figs 6a and b, the pressure distribution on the different building areas, for the studied wind directions, are displayed. Common features of the pressure distributions are listed below.

● A positive pressure is found on the wind exposed areas. Maximum pressure zones (stagnation zones) can be seen on the upper, central parts of the windward walls and on the lower, central part of the windward roof (Fig. 6). On the other building areas, negative pressure is found. The maximum negative pressure is found just behind the front corners of the house.

In Figs 7 and 8, a comparison between calculated and measured pressure distribution on a horizontal level and vertical section is made. The figures show that the calculated values, in a systematic way, are higher than the measured ones. This tendency is also confirmed in Tables 1 and 2, where the area average pressure coefficients are shown.

3.3. *A house surrounded by identical houses*

In Figs 9a and b, the pressure coefficient distributions for the two wind directions are shown. In principal, the main features here are the same as the ones presented for the single house. A few differences are however noteworthy.

● The zone of maximum pressure is now found at the outer parts of the wind exposed frontal house areas. This in contrast to the position of the zone for a single house, which was in the central parts of the windward wall.

● On the most downstream parts of the side walls, the pressure coefficient is now positive. For the single house

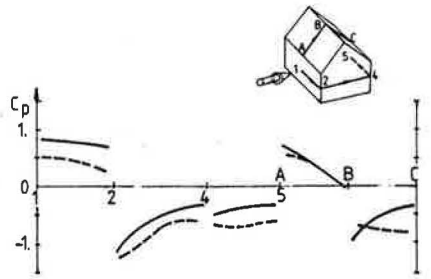

Fig. 7. Calculated (——) and wind tunnel measured (– – –) distribution of c_p at one horizontal level and vertical section of a single house. Wind towards the longside wall.

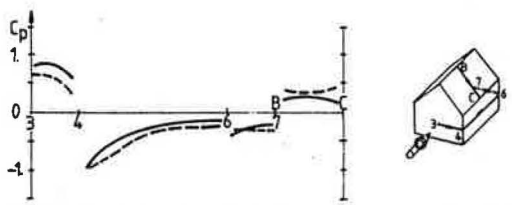

Fig. 8. Calculated (——) and wind tunnel measured (– – –) distribution of c_p at one horizon level and vertical section for a single house. Wind towards the gable wall.

Table 1. Average pressure coefficients for different building areas. (a) wind against the longside wall; (b) wind against the gable wall. The single house.

	Average pressure coefficient				
(a)	Windward wall	Leeward wall	Gable wall	Windward roof	Leeward roof
Numerical calculations	0.8	−0.4	−0.6	0.3	−0.9
Wind tunnel measurements	0.5	−0.7	−0.9	0.3	−0.8
	Average pressure coefficient				
(b)	Windward gable	Leeward gable	Longside wall	Roof	—
Numerical calculations	0.8	−0.3	−0.3	−0.5	—
Wind tunnel measurements	0.6	−0.3	−0.5	−0.6	—

the entire side wall was exposed to a negative pressure coefficient.

In Figs 10 and 11, and in Table 2, where the comparison with the wind tunnel data are shown for this case. The tendency is the same as for the case of the single house. The calculated pressure coefficients are generally higher than the measured ones.

4. DISCUSSION AND CONCLUSIONS

The numerical simulations of the pressure field around the three dimensional building which are presented in this paper can be characterized as introductory studies. The main purpose of this work was to investigate if a numerical model, from an engineering point of view, can be used to obtain information about the pressure and flow field around relatively complicated buildings.

The results presented in this work indicate that the numerical model gives a realistic description of the pressure field around a house, when compared with wind tunnel measurement. There are differences between calculated and measured pressure values. The differences are essentially quantitative. From a qualitative point of view the calculations show rather good agreement with measurements. A few comments on the results are given below.

It is believed that the differences between predicted and measured pressure fields can to a large extent be attributed to uncertain boundary conditions. In particular the velocity distribution and turbulence intensity of the approaching boundary layer are expected to be crucial. A systematic variation of the turbulence intensity in the approaching boundary layer and its effect on the pressure fields has been reported by Barriga *et al.* [8], see Fig. 12. The conclusion to be drawn is that the frontal pressure level is not affected by a change in turbulence intensity, while the leeward side shows a clear sensitivity. The sensitivity to the velocity distribution was evaluated, by way of a numerical experiment, in the present work, see Fig. 13. It was found that the pressure level on the frontal wall shows a strong sensitivity to the velocity distribution, while the leeward side is less sensitive. The results, both the sensitivity to turbulence intensity and velocity distribution, are to be expected when considering that the frontal side pressure is mainly balancing the velocity head of the approaching wind and that the leeward side pressure is related to the shear layer development behind the obstacle. In the wind tunnel measurements used for comparison in the present study

Table 2. Average pressure coefficients for different building areas. (a) wind against the longside wall; (b) wind against the gable wall. The house situated in a group of identical houses.

	Average pressure coefficient				
(a)	Windward wall	Leeward wall	Gable wall	Windward roof	Leeward roof
Numerical calculations	0.3	−0.1	−0.1	0.3	−0.4
Wind tunnel measurements	0.1	−0.3	−0.3	0.1	−0.4
	Average pressure coefficient				
(b)	Windward gable	Leeward gable	Longside wall	Roof	—
Numerical calculations	0.3	−0.2	−0.1	−0.1	—
Wind tunnel measurements	0.2	−0.2	−0.2	−0.2	—

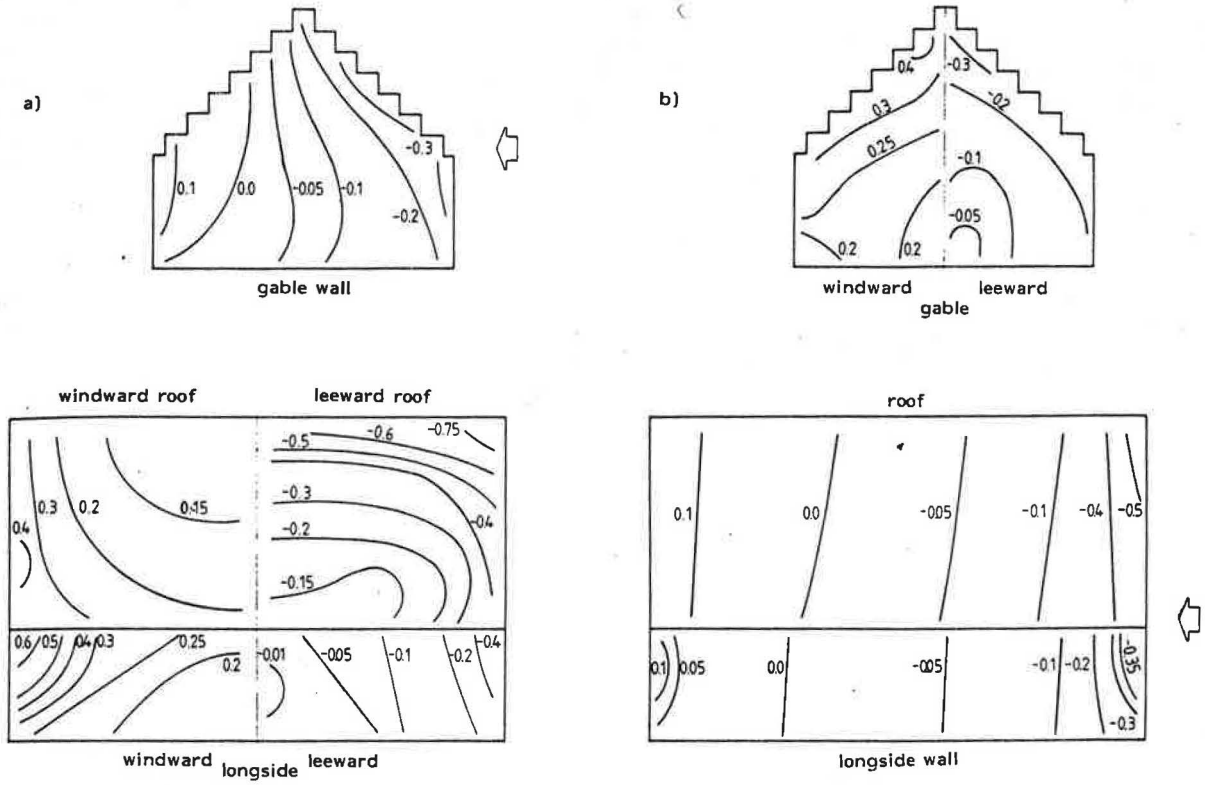

Fig. 9. Distribution of the pressure coefficient (c_p) on the surface of a house in a group. Wind direction: (a) towards the longside wall; (b) towards the gable wall.

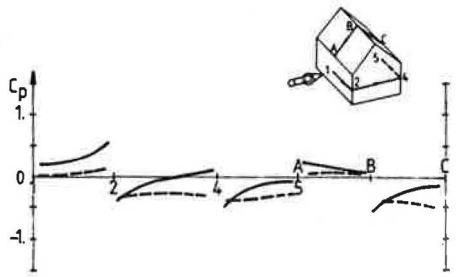

Fig. 10. Calculated (——) and wind tunnel measured (– – –) distribution of c_p at one level and section for a house in a group. Wind towards the longside wall.

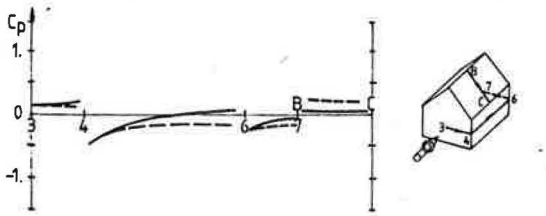

Fig. 11. Calculated (——) and wind tunnel measured (– – –) distribution of c_p at one level and section for a house in a group. Wind against the gable wall.

"background" profiles of velocity and turbulence intensity were measured at the measuring section in the wind tunnel, far away from where the boundary conditions in the numerical model were applied. Uncertainties are thus introduced which should be kept in mind when comparing the predictions and the measurements.

Current development of the numerical model pre-

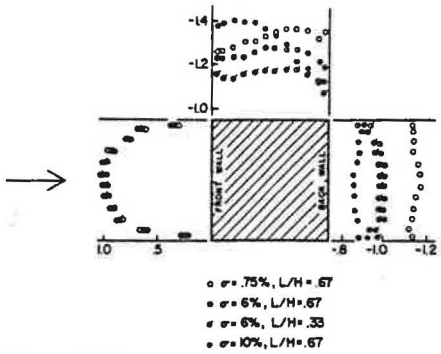

Fig. 12. Effect of turbulence intensity and scale on the pressure coefficient distribution on a square cylinder. After [8].

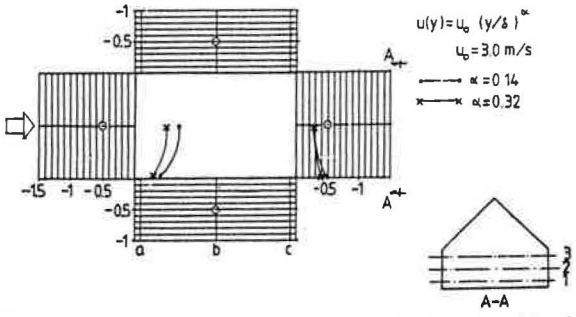

Fig. 13. Pressure coefficient distribution at the horizontal level 2 for two different inlet velocity profiles.

sented is directed towards improved resolution by the numerical grid. By using a body-fitted coordinate system (BFC) a detailed resolution of complex buildings and surrounding topography is within reach. Three-dimensional applications have already been carried out, and an example is given in Fig. 14. The grid is seen to follow the curved shape of the building smoothly. We expect the BFC grids to be a major improvement that will make it possible to perform high resolution predictions.

Finally, the following conclusions:

- The results obtained with the numerical model regarding the pressure field around a house are generally good from an engineering point of view.
- Differences as compared to the wind tunnel experiments exist, but they are explicable and probably relatively easy to decrease using, for example, improved boundary conditions.

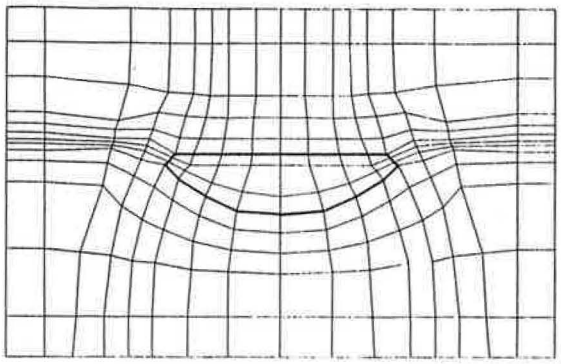

Fig. 14. Example of the application of a BFC grid. Plane view.

Acknowledgement—The work reported here has been sponsored in part by the Swedish Council for Building Research under grant No. 851092-6 to the Swedish Meteorological and Hydrological Institute.

REFERENCES

1. T. Hanson, D. M. Summers and C. B. Wilson, Numerical modelling of wind flow over buildings in two dimensions. *Int. J. Numerical Meth. Fluids* **4**, 24–41 (1984).
2. D. M. Summers, T. Hanson and C. B. Wilson, Validation of a computer simulation of wind flow over a building model. *Bldg Envir.* **21**, 97–111 (1986).
3. D. A. Paterson and C. J. Apelt, Computation of wind flows over three-dimensional buildings. *J. Wind Engng Ind. Aerodyn.* **24**, 193–213 (1986).
4. W. Rodi, Turbulence models and their application in hydraulics—a state of the art review (IAHR). University of Karlsruhe, Karlsruhe, F.R.G. (1980).
5. D. B. Spalding, A general purpose computer program for multi-dimensional one- and two-phase flow. *Math. Comput. Simulation* **8**, 267–276 (1981).
6. B. G. Wirén, Effects of surrounding buildings on wind pressure distributions and ventilation losses for single-family houses. Part 1: 1½-storey detached houses. Meddelande M85:19. Statens Institut för Byggnadsforskning. (1985).
7. O. Zeman and H. Tennekes, A self-contained model for the pressure terms in the turbulent stress equations of the neutral atmospheric boundary layer. *J. Atmosph. Sci.* **32**, 1808–1813 (1975).
8. A. R. Barriga, C. T. Crowe and J. A. Roberson, Pressure distribution on a square cylinder at a small angle of attack in a turbulent cross flow. Proceedings of the Fourth International Conf. on Wind Effects on Buildings and Structures (1975).